which the measured data represents actual two-dimensional flow. Figure 1 shows this comparison for an angle of attack of 5°, and indicates quite good agreement. This agreement was improved at low angles of attack and was poorer at the higher angles when separation altered the two-dimensional nature of the flow.

Conclusions

A rotating cylinder at the leading edge of a lifting body can effectively control boundary-layer separation as evidenced by experimental results. The upper limit on the angle of attack without separation was a result of boundary-layer accumulation on the wind-tunnel walls and consequently does not represent a limitation in applications. Also, the two-dimensional configuration as tested presents higher adverse pressure gradients and thus a more difficult boundary-layer control application than a lifting body having finite span. The gap between the cylinder and the fixed afterbody has been shown to be a significant parameter. This gap should be maintained at its minimum practical value in order to minimize the cylinder speed required for effective boundary-layer control.

References

[1] Thwaites, B., ed., *Incompressible Aerodynamics,* Clarendon Press, Oxford, 1960. p. 215.

[2] Goldstein, S., ed., *Modern Developments in Fluid Dynamics,* Clarendon Press, Oxford, 1938. p. 78.

[3] Farve, M.A., "Un nouveau procede hypersustenateur: l'aile a' parol d' extrados mobile," *Mechanique Expermentale Des Fluids,* Comtes Rendus, 1934. p. 634.

[4] Alvarez-Calderon, A., and Arnold, F.A., "A Study of the Aerodynamic Characteristics of a High-Lift Device Based on a Rotating Cylinder Flap," Tech. Rept. RCF-1, Sept. 1961, Stanford University, Stanford, Calif.

[5] Tennant, J.S., "A Subsonic Diffuser With Moving Walls for Boundary Layer Control," *AIAA Journal,* Vol. 11, Feb. 1973, p. 240.

[6] Steele, B.N. and Harding, M.H., "The Application of Rotating Cylinders to Ship Maneuvering," National Physical Laboratory (Britain) Ship Rept. 148, Dec. 1970.

[7] Smith, A.M.O., "Exact Solution of the Newman Problem. Calculation of Non Circulatory Plane and Axially Symmetric Flows About or Within Arbitrary Boundaries," Rept. ES 26988, April 1958, Douglas Aircraft Co., Long Beach, Calif.

Calculations of the Turbulent Wake Behind Slender Self-Propelled Bodies with a Kinetic Energy Method

Roy C. Swanson Jr.* and Joseph A. Schetz†
Virginia Polytechnic Institute and State University
Blacksburg, Va.

Nomenclature

a_1 = factor in Eq. (1)
D = diameter
k = turbulent kinetic energy
U = axial velocity
U_E = freestream velocity
U_C = centerline velocity
X = axial coordinate
ρ = density
τ = shear
$-\overline{u'v'}$ = Reynolds stress

Received January 13, 1975. This work was supported by the Advanced Research Projects Agency. Technical monitoring was by the Office of Naval Research.

Index categories: Jets, Wakes, and Viscid-Invisoid Flow Interaction; Viscous Nonboundary-Layer Flows; Marine Hydrodynamics, Vessel and Control Surface.

*Graduate Research Assistant, Aerospace and Ocean Engineering Department, now at Naval Surface Weapons Center.

†Professor and Department Chairman, Aerospace and Ocean Engineering Department. Associate Fellow AIAA.

Introduction

THERE has been a relative scarcity of experimental and theoretical information on the behavior of turbulent wakes behind self-propelled bodies. An extensive experimental program concerning slender bodies at high Reynold's number ($Re_D \approx 600{,}000$) has recently been completed and reported in Refs. 1-3. There were three models studied, all with the same forebody shape. The first (Model#1) was simply a drag-body with a sharp stern. Model #2 was self-propelled by means of axial injection through a peripheral slot, and Model #3 was driven by a propeller.

To complement these experiments, calculations of wake development were made using the kinetic energy formulation of Harsha,[4] and this Note serves to report the results of that undertaking. Some modifications to the basic approach were found necessary[4] to handle the momentumless cases. A key relationship in the formulation is that between shear τ and the local kinetic energy k, and for normal free shear flows the following has been employed

$$\tau = a_1 \rho k \tag{1}$$

where ρ is the density and $a_1 = 0.3$. Although a_1 can be taken as a constant value of 0.3 over most of the wake flow, it is not a constant in the vicinity of the centerline since the shear stress vanishes at that point for axisymmetric flows; in this program we have used[4]

$$a_1 = 0.3 \frac{\partial U/\partial R}{|\partial U/\partial R|_{\max}} \tag{2}$$

for normal shear flows, i.e., Model #1. This relation was applied from the centerline to the point $\partial U/\partial R = (\partial U/\partial R)_{\max}$. Beyond that point

$$a_1 = 0.3 \frac{\partial U/\partial R}{|\partial U/\partial R|} \tag{3}$$

which yields the proper sign. To avoid an excessive shear stress value in the outer region of the flow for momentumless cases, the program was modified[4] to include the following formulation:

$$a_1 = 0.3 \frac{\partial U/\partial R}{|\partial U/\partial R|_{\max}} \quad \partial U/\partial R > 0$$
$$a_1 = 0.3 \frac{\partial U/\partial R}{|(\partial U/\partial R)_{\min}|} \quad \partial U/\partial R < 0 \tag{4}$$

Complete information on modeling of the other terms in the turbulent kinetic energy equation, i.e., dissipation and diffusion terms, is provided in Ref. 5. Note, all parameters involved in modeling were taken as the normal values, as dictated by previous experiments, generally not momentumless. This was necessary since our recent experimental effort did not penetrate the regime of statistical flow characteristics, i.e., turbulence length scale, autocorrelation functions, and energy spectrum.

Results

Since the formulation is parabolic, the principal information required to undertake a calculation is in the form

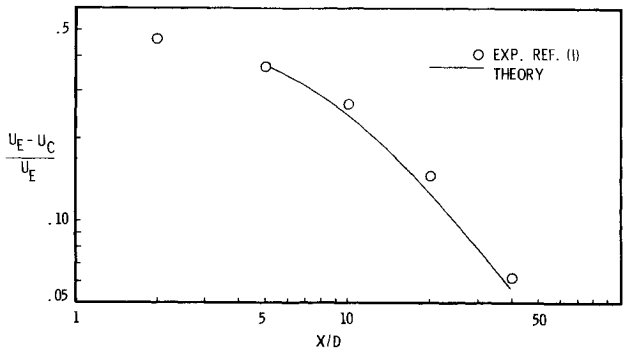

Fig. 1 Axial velocity deficit vs X/D—model #1.

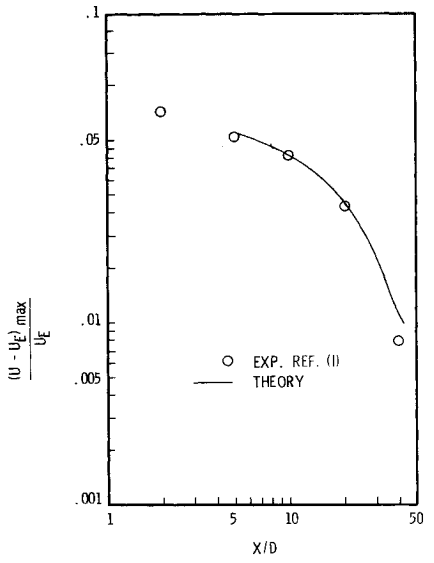

Fig. 2 Maximum axial velocity excess vs X/D—model #2.

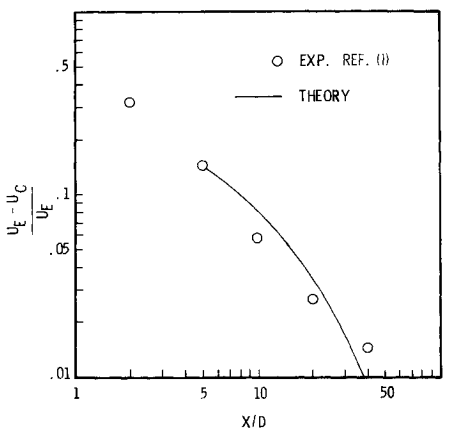

Fig. 3 Axial velocity deficit vs X/D—model #3.

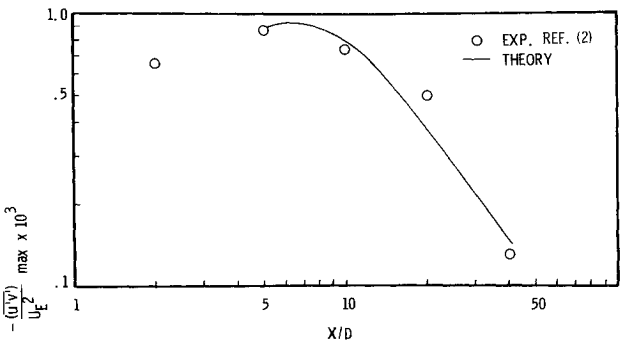

Fig. 4 X/D decay of maximum shear stress—model #1.

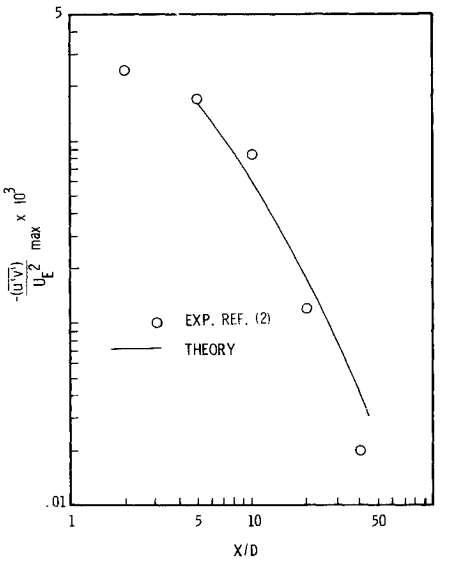

Fig. 5 X/D decay of maximum shear stress—model #3.

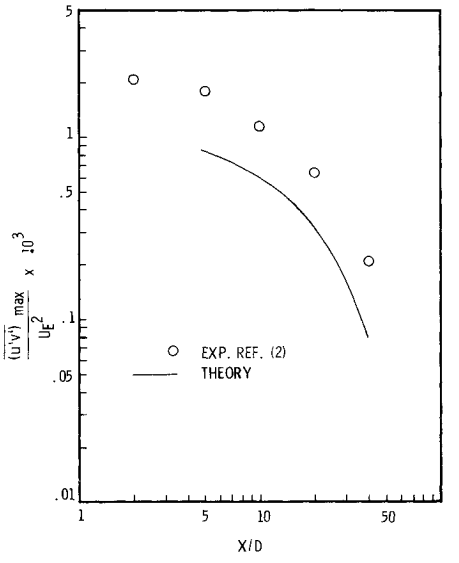

Fig. 6 X/D decay of maximum shear stress—model #2.

of initial conditions. These were taken from the experimental measurements at $X/D=5$. This included not only the radial distributions of the dependent variables, but also an initial eddy viscosity distribution which was obtained from the measured shear stress and velocity distributions. For Model #2, this procedure produced results in strong disagreement with the data, so an alternate calculation using a constant initial eddy viscosity of 0.072 suggested by Naudascher's[6] data was attempted.

This computer routine did not include a tangential momentum equation, so that swirl is not accounted for, and the calculations for Model # 3 are not exact and must be interpreted carefully. The principal calculations were begun at $X/D=5$, since the swirl velocity has decayed to a low value at that station.[1] It is significant, however, that calculations begun at $X/D=10$ and 20 showed the same trends even though the swirl velocity had decayed to even lower values by those stations.[1]

For Model #1 the numerical prediction of the downstream decay of the centerline mean velocity deficit, as shown in Fig. 1, agrees well with the experimental results. Even though the

actual values are slightly underestimated, the rate of decay is followed very closely. The calculations for Model #2 shown in Fig. 2 are those made with the initial conditions on eddy viscosity obtained from Naudascher's work. They demonstrate reasonable agreement with the data. However, there is a tailing-off of the numerical solution in the $X/D=40$ region; this was caused by the mass entrainment model used.

As for Model #3, the numerical computations overpredict the experimental values initially, and the rate of decrease of velocity deficit is considerably greater than that suggested by the data when $X/D=40$ is reached (Fig. 3). The main reason probably lies in the lack of statistical turbulence data for this kind of flow, upon which to base refinements in the kinetic energy model.

The TKE program also provided the streamwise variation in radial shear stress for each of the models. The computations for Models #1 and #3, as depicted in Figs. 4 and 5, respectively, show fairly good agreement with experiment; however, the rates of decay are lower than they should be. In the case of Model #2, the trend shown follows that exhibited by the experiment, but the values are underpredicted (Fig. 6). Of course, the initial value for Model #2 is not matched since the initial conditions were artificially adjusted as previously described.

Conclusions

The kinetic energy method, and the specific formulation of Harsha, have been shown to be of value in predicting the wake behind slender bodies in both the drag and self-propelled modes. Not surprisingly, the best agreement between numerical prediction and experiment was obtained for the drag body case. Agreement of a precision adequate for any engineering task was readily obtained for that case.

Of the two self-propelled cases, the better agreement between prediction and experiment was found for the propeller-driven case. This was surprising, since the numerical procedure used did not include swirl, and the experiment certainly did, although it had decayed to a low value in the range of X/D considered here. Reasonable agreement for the jet-propelled case could only be obtained by tampering with the initial conditions on the eddy viscosity. The reasons for our difficulty in treating this flow situation with the kinetic energy method are not known. Presumably some structural differences in the turbulence field exist which were not properly modeled in the usual approach. Finally, it should be noted that the Harsha code is easy and convenient to use. It is also quite well documented.

References

[1] Swanson, Jr., R. C., Schetz, J. A., and Jakubowski, A. K., "Turbulent Wake Behind Slender Bodies, Including Self-Propelled Configurations," VPI Report Aero-024, Sept. 1974, Virginia Polytechnic Institute and State University, Blacksburg, Va., available through DDC.

[2] Chieng, C. C., Jakubowski, A. K., and Schetz, J. A., "Investigation of the Turbulent Properties of the Wake Behind Self-Propelled Axisymmetric Bodies," VPI Rept. Aero-025, Sept. 1974, Virginia Polytechnic Institute and State University, Blacksburg, Va., available through DDC.

[3] Schetz, J. A. and Jakubowski, A. K., "Experimental Studies of the Turbulent Wake Behind Self-Propelled Slender Bodies," Paper 75-117, Pasadena, Calif.

[4] Harsha, P. T., private communication.

[5] Harsha, T., "Prediction of Free Turbulent Mixing Using a Turbulent Kinetic Energy Method," *Proceedings of the 1972 NASA-Langley Working Conference on Free Turbulent Mixing*, SP-351, NASA.

[6] Naudascher, E., "Flow in the Wake of Self-Propelled Bodies and Related Sources of Turbulence," *Journal of Fluid Mechanics*, Vol. 22, pt. 4, 1965, pp. 625-656.